Bioorganic & Medicinal Chemistry 18 (2010) 855–862

Contents lists available at ScienceDirect

Bioorganic & Medicinal Chemistry

journal homepage: www.elsevier.com/locate/bmc

# Design, synthesis and biological evaluation of 6-(benzyloxy)-4-methylquinolin-2(1*H*)-one derivatives as PDE3 inhibitors

Mohsen Nikpour [a], Hamid Sadeghian [b,*], Mohammad Reza Saberi [c], Reza Shafiee Nick [d], Seyed Mohammad Seyedi [e], Azar Hosseini [d], Heydar Parsaee [d], Alireza Taghian Dasht Bozorg [a]

[a] Department of Chemistry, School of Sciences, Islamic Azad University, Ahvaz Branch, Ahvaz, 61349-68875, Islamic Republic of Iran
[b] Department of Laboratory Sciences, School of Paramedical Sciences, Mashhad University of Medical Sciences, Mashhad, Islamic Republic of Iran
[c] School of Pharmacy, Pharmaceutical Research Center, Mashhad University of Medical Sciences, BuAli Square, Mashhad 91857-63788, Islamic Republic of Iran
[d] Department of Pharmacology, School of Medicine, Pharmacological Research Center of Medicinal Plants, Mashhad University of Medical Sciences, Mashhad, Islamic Republic of Iran
[e] Department of Chemistry, School of Sciences, Ferdowsi University of Mashhad, Mashhad, Islamic Republic of Iran

ARTICLE INFO

*Article history:*
Received 22 October 2009
Revised 19 November 2009
Accepted 20 November 2009
Available online 26 November 2009

*Keywords:*
Inotropic
Vesnarinone
Chronotropic
Rat atria
Docking

ABSTRACT

Selective PDE3 (phosphodiesterase 3) inhibitors improve cardiac contractility and may be used in congestive heart failure. However, their proarrhythmic potential is the most important side effect. In this work ten new synthetic compounds (3-[(4-methyl-2-oxo-1,2-dihydro-6-quinolinyl)oxy]methylbenzamide analogs: **4a**–**j**) were designed, synthesized and tested for the inhibitory activity against human PDE3A and PDE3B. The strategy of the design was based on the structure of vesnarinone (a selective PDE3 inhibitor) and its docking analysis results. The synthetic compounds showed better PDE3 inhibitory activity in comparison with vesnarinone. Using docking analysis, a common binding model of each compound toward PDE3 was suggested. In the next step the potential cardiotonic activity of the best PDE3A inhibitors (**4b**, $IC_{50} = 0.43 \pm 0.04$ μM) was evaluated by using the spontaneously beating atria model. In the experiment, atrium of reserpine-treated rat was isolated and the contractile and chronotropic effects of the synthetic compound were assessed. That was carried out in comparison with vesnarinone. The best pharmacological profile was obtained for the compound **4b**, which displayed selectivity for increasing the force of contraction (46 ± 3% change over the control) rather than the frequency rate (16 ± 4% change over the control) at 100 μM.



## 1. Introduction

Congestive heart failure (CHF) is a major cause of death in patients with heart disease. Digitalis glycosides have been used for the treatment of CHF for many years. However, application of these agents is limited because of their narrow therapeutic window and their propensity that cause life-threatening arrhythmias (arrhythmogenic lability). The literature survey for orally active 'non-glycoside' cardiotonic drugs displays a greater safety profile and improved efficacy on patient survival that resulted in establishing the selective inhibitors of cyclic nucleotide phosphodiesterase (PDE) enzymes as a new class of cardiotonic agents.

PDE enzymes specifically hydrolyze cAMP (cyclic adenosine monophosphate) and cGMP (cyclic guanosine monophosphate) in the cells. On the basis of their amino-acid sequence homology, biochemical properties and inhibitor profiles, 11 PDE families have been recognized in mammalian tissues, PDE1, PDE2 to PDE11. Each PDE isozyme has a C-terminal catalytic domain conserved throughout the family, and an N-terminal regulatory domain unique for each isozyme. They are expressed in tissue and cell-specific distribution patterns, and they show different substrate affinities and inhibitor sensitivities.[1] Most cell types express one or more PDE isozymes, each regulating intracellular cAMP and/or cGMP concentrations in different cellular compartments and in different manners. In cardiovascular tissues, PDE3 and PDE4 are well established as the dominant cAMP-hydrolysis isozymes.[2] PDE1, PDE3, PDE4, and PDE5 are expressed in aortic smooth muscle cells;[3,4] PDE1, PDE2, PDE3, and PDE4 are expressed in the heart,[5] whereas PDE2, PDE3, and PDE5 are found in platelets.[2,6,7] PDE3 is thus a unique cAMP-regulating isozyme expressed in all of mentioned tissues. These tissues contribute significantly to the pathogenesis of arteriosclerosis obliterans and restenosis after angioplasty. It was shown that the inhibition of PDE3 activity in cardiovascular tissues resulted in increasing the levels of cAMP with consequent reduction in platelet aggregation and smooth muscle cell proliferation in vitro, and induction of a cardiotonic effect.[7,8]

The PDE3 subfamily consists of two closely related subtypes: PDE3A and PDE3B. PDE3A is mostly expressed in cardiac tissue,

* Corresponding author. Tel.: +98 05117610111; fax: +98 05117628088.
*E-mail addresses:* sadeghianh@mums.ac.ir, hd_sn@yahoo.com (H. Sadeghian).

0968-0896/$ - see front matter © 2009 Elsevier Ltd. All rights reserved.
doi:10.1016/j.bmc.2009.11.044

platelets, and vascular smooth muscle cells, while PDE3B is prevalently expressed in hepatocytes and adipose tissue.[9,10]

Vesnarinon (3,4-dihydro-6-[4-(3,4-dimethoxybenzoyl)-1-piperazinyl]-2(1*H*)-quinolinone) (Fig. 1) was documented as an effective inotropic agent for treating congestive heart failure.[11,12] This compound increases contractility by inhibiting phosphodiesterase III activity and prolonging the potential action duration via increasing inward $Ca^{2+}$ currents and inhibiting repolarizing $K^+$ currents.[13] Also vesnarinone has demonstrated a unique spectrum of intriguing biologic effects, including tumor cell differentiating and proapoptotic properties.[14] Clinical application of vesnarinone is restricted because of the severe side effect of agranulocytosis.[15]

Despite considerable research efforts towards providing insights into PDE3–ligand interactions,[16–19] the progress in this area still relies heavily on information about structure–activity relationships (SAR) collected from identification of new ligands that were discovered by trial and error. Using computerized study of PDE3–ligand interaction, we designed and synthesized new series of cardiotonic agents by modifying the structure of vesnarinone. Afterward, the inhibitory activities of the synthetic compounds were measured against PDE3A and PDE3B and the potential cardiotonic activity of the best PDE3A inhibitors was assessed.

## 2. Results and discussions

In order to give further proof to the mechanism of action of designed inhibitors, molecular models of the complex enzyme–inhibitor were generated for both ligands and vesnarinone, using PDE3B co-crystalized with MERCK1[19] and the site-directed mutagenesis data available for PDE3A.[17,20–23]

There is reasonable homology between the PDE3A and PDE3B (identities: 48%, positives: 67%, extracted from NCBI-BLAST[24–26]). This homology increases (~95%) within 15 Å in the active site pocket.[27]

The lactamic portion of vesnarinone was supposed to be the primary binding moiety and as common anchor point. A similar case was confirmed by Scapin et al. for cilostamide, cilostazol and amrinone (Fig. 1).[19]

We generated 100 docked conformers of vesnarinone in ADT software. A detailed assessment of each conformers (all of the 100 docked models) revealed that more than 50% of docking results had nearly identical orientations in which: (1) quinolinone group of inhibitors oriented toward $Glu^{988}$, (2) piperazine moiety was flanked by the hydrophobic portions of the $Leu^{895}$, $Ile^{938}$, $Ile^{955}$, and $Phe^{991}$ side chain and (3) dimethoxybenzamide moiety was surrounded by $His^{737}$, $His^{825}$ and $Thr^{829}$ side chains. Due to the orientation mentioned, the docked conformers displayed hydrogen bond with the amide group of $Gln^{988}$ side chain in PDE3B while the 4-(3,4-dimethoxybenzoyl)-1-piperazinyl moiety, as the second bonding part of vesnarinone, interact with pocket formed by residues: $Tyr^{736}$, $His^{737}$, $His^{825}$, $Thr^{829}$, $Leu^{895}$, $Ile^{938}$, $Ile^{955}$, $Phe^{959}$, $Leu^{987}$ and $Phe^{991}$ (Fig. 2). The importance of the mentioned amino acids in catalytic activity of the PDE3 has been proved by site direct mutagenesis[17,21,22] and multiple alignment technique.[27] In previous work we found that by placing methyl group in position 4 of carbostiryl moiety, the PDE3 inhibitory activity of the compounds increases. In order to obtain new vesnarinone analogs with a better PDE3 inhibitory activity, we planned to substitute 4-methyl group on 6-hydroxycarbostiryl and to replace piperazine with benzamide moiety (Fig. 3). In the later modification, the hydrophobic interaction with side chain of $Leu^{895}$, $Ile^{938}$, $Ile^{955}$, and $Phe^{991}$ increases. Among the mentioned residues $Phe^{991}$ is the most critical amino acid over all species so that in PDE3A, $Phe^{1004}$→Ala mutant ($Phe^{1004}$ is the homolog of $Phe^{991}$ in PDE3B[27]) decreased the catalytic efficiency ($k_{cat}/K_m$) by 286-fold from wild type enzyme.[22] On the basis of the mentioned hypothesis (modifying the structure of vesnarinone), compounds **4a** and **4a**′ was designed, synthesized and their PDE3 (types A and B) inhibitory activities was assessed in comparison with vesnarinone. Among the three compounds, **4a** was the most potent inhibitors. The $IC_{50}$ value of **4a** was lower than vesnarinone by six and four-fold for PDE3A and PDE3B, respectively (Table 2). The results of Table 2 indicate that the substitution of 4-methyl on 6-hydroxycarbostiryl moiety will lead to an increase in inhibitory activity.

Considering the inhibitory activity of **4a**, other analogs were designed. Binding affinity of designed molecular structures (compounds **4a–j**) toward PDE3A and PDE3B was studied. 100 Docked conformers of **4a–j** were generated in ADT software. A detailed assessment of each conformer (all of the 100 docked models) revealed that more than 30% of docking results had nearly identical orientations towards suggested inhibitory model of docked vesnarinone. The most mimic conformer with vesnarinone at lowest $K_i$ was adopted from each 100 docked models as the 'consensus' structure and then used for further analysis (Fig. 4). The calculated $K_i$ for the consensus structure of the mentioned compounds was in a good range of 10e-8 to 10e-10 μM (Table 1). Therefore other analogs of **4a** (compounds **4b–j**) were synthesized and their inhibitory activity against human PDE3A and PDE3B was tested.

The synthetic compounds **4a–j** showed a short range of inhibition activity against the two enzymes ($IC_{50}$ = 0.43–1.76 μM for PDE3A and $IC_{50}$ = 0.91–3.50 μM for PDE3B; Table 2). The synthetic compounds showed a better inhibitory activity against PDE3A in comparison with PDE3B while **4b** having a 4-methylpiperidine substituent was the most potent inhibitor of PDE3A at 0.43 μM. Considering the $IC_{50}$ values in Table 2, there is no satisfactory relationship between $IC_{50}$ values of PDE3B and $K_i$ of proposed bonding conformation of docking study. To earn the best bonding conformation for these series of compounds, further analysis on docking results was tried.

Docking procedure was carried on several times in order to find the best fitness between experimental and docking results. Sometimes, we had to increase the generation number to more than 250 to get the proper conformer of ligand. This is aligned with other synthetic compounds in the same direction up to keeping the minimal accepted $K_i$ value. The result of this strategy was so satisfactory that there was at least one conformer in proper orientation and proper $K_i$ value for each ligand (Fig. 4).

Figures 2 and 4 show that the inhibitors could interact with the active site in quite opposite direction than that reported by

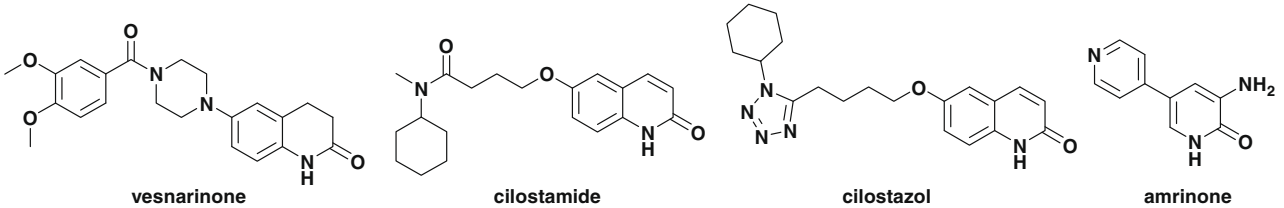


**Figure 1.** Chemical structure of some PDE inhibitors.

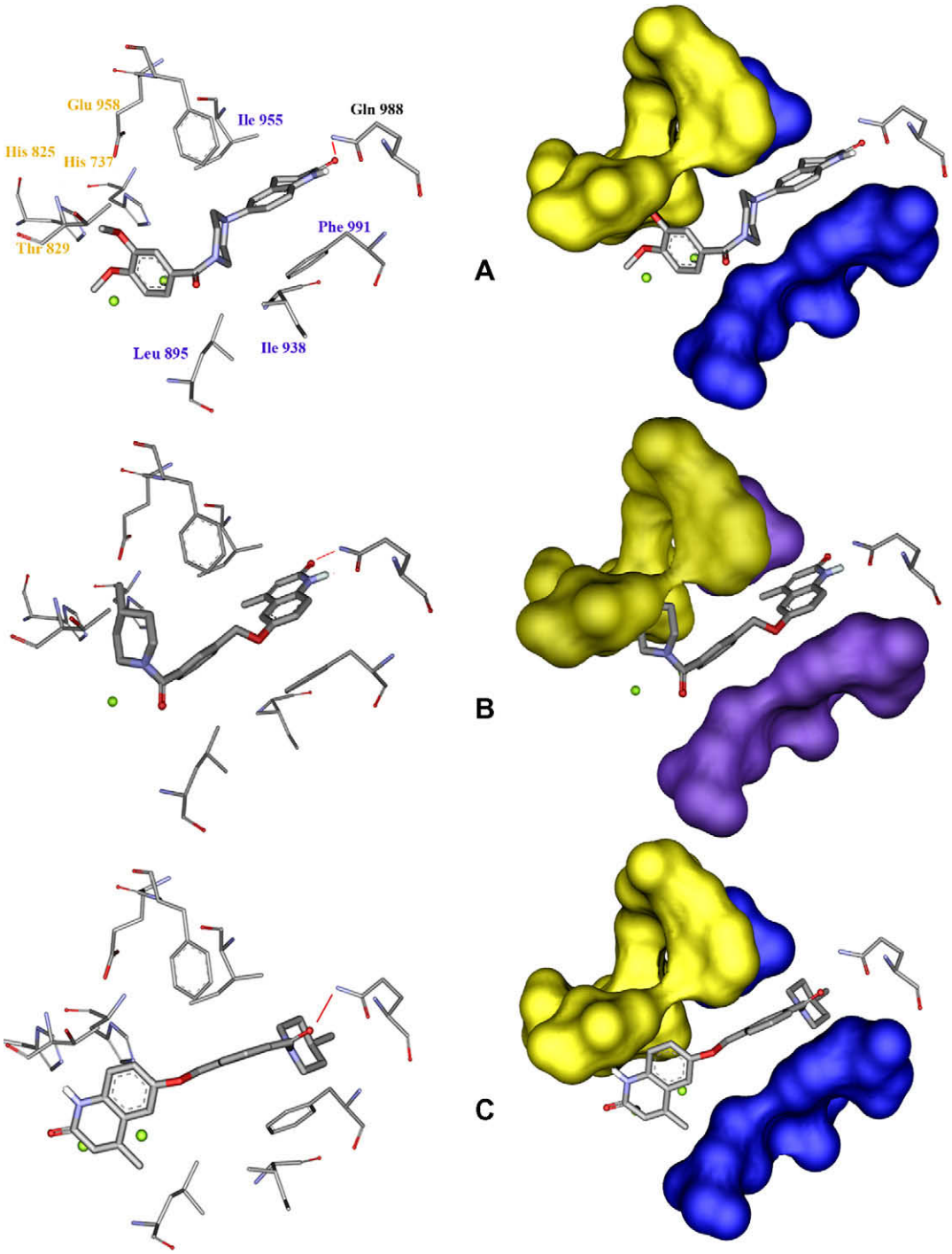


**Figure 2.** Stick (left) and solvent surface (right) view of the amino acids interacted with vesnarinone (A), **4b** in traditional orientation (B) and **4b** in new proposed orientation (C). The residues which have intermolecular interactions with amide and piperazine moiety of vesnarinone were distinguished by yellow and blue color, respectively. In this figure hydrogen bonds of $Gln^{988}$ with the docked structures are shown in red line.

Scapin et al.[19] while the $K_i$ is still in a proper range. In this orientation consensus structures of the docked compounds show hydrophobic interaction with $Phe^{991}$ via their phenyl portion and hydrogen bond with highly conserved $His^{825}$ and $Gln^{988}$ via quinolinone and benzamide portions, respectively (Fig. 4). It is notable that mutant $His^{840}$→Ala in PDE3A lead to no catalytic activity even at high concentration of the mutated enzyme.[20] Considering the high identity (~95%) between PDE3A and PDE3B, the catalytic role of $His^{840}$ in PDE3A can be extended to its homolog $His^{825}$ in PDE3B. Both residues are conserved among all PDEs.[27] In PDE3B, $His^{825}$ directly bind to the magnesium ion which is involved in hydrolysis.[19] The direct linear relation between $-\log K_i$ and $-\log IC_{50}$ of PDE3B proved the proposed direction for the inhibitors in the active site of the enzyme (Fig. 5). It became more clear when two series of orientations were compared in which, graph A showed the $K_i$ for aforementioned proposed orientation while graph B represented the $K_i$ for our proposed orientation against $IC_{50}$ (Fig. 5). There was not any acceptable line for graph A while there was a suitable line for graph B with 0.96 regressions.

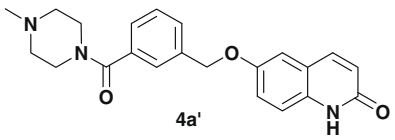


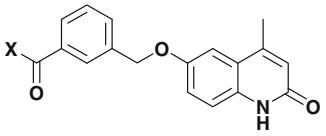

| X | Compd. | X | Compd. |
|---|---|---|---|
| 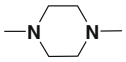 | 4a | 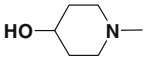 | 4f |
| 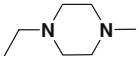 | 4b |  | 4g |
| 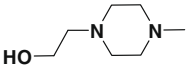 | 4c | 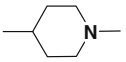 | 4h |
| 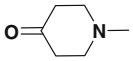 | 4d | 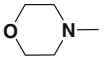 | 4i |
| 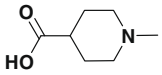 | 4e |  | 4j |

**Figure 3.** The structure of amide moiety of compounds **4a–j** and **4a**′.

**Table 1**
Docking analysis data of consensus conformers

| Compd | $K_i^*$ | $\Delta G_b^*$ | $E_d^*$ | $K_i$ | $\Delta G_b$ | $E_d$ |
|---|---|---|---|---|---|---|
| **4a** | 5.05e−9 | −11.32 | −13.01 | 3.55e−8 | −10.16 | −11.41 |
| **4b** | 1.43e−9 | −12.07 | −13.92 | 1.37e−8 | −10.73 | −12.06 |
| **4c** | 5.68e−10 | −12.61 | −14.61 | 2.01e−8 | −10.50 | −12.08 |
| **4d** | 4.50e−8 | −10.04 | −11.90 | 1.37e−8 | −10.73 | −12.05 |
| **4e** | 3.50e−8 | −10.17 | −12.09 | 8.94e−9 | −10.98 | −11.77 |
| **4f** | 2.37e−8 | −10.40 | −11.30 | 6.37e−9 | −11.18 | −12.41 |
| **4g** | 3.72e−8 | −10.14 | −11.69 | 1.36e−8 | −10.73 | −11.35 |
| **4h** | 8.64e−9 | −11.00 | −12.62 | 1.23e−8 | −10.79 | −12.27 |
| **4i** | 5.24e−8 | −9.93 | −11.73 | 1.04e−8 | −10.89 | −12.08 |
| **4j** | 7.64e−8 | −9.71 | −11.01 | 5.02e−8 | −9.96 | −11.07 |

$\Delta G_b$: estimated free energy of bonding, $E_d$: final docking energy, $K_i$: estimated inhibition constant. The docking parameters distinguished with * related to traditional orientation.

We also investigated other possible orientations which might be candidate for interaction with the active site of PDE3B. There was no relation between the $K_i$ and $IC_{50}$ values.

In light of PDE3A as mostly expressed in cardiac tissue versus PDE3B, compound **4b** which had showed the best PDE3A inhibitory activity was tested for its effect on the force of contraction and frequency rate of rat spontaneously beating atria in comparison with vesnarinone. To avoid bias of catecholamine release, we used preparations obtained from reserpine-pretreated animals.

Compound **4b** which was the most active PDE3A inhibitor increased the atrial contractility nearly equal to vesnarinone (46 ± 3% vs 41 ± 3% increases at 100 μM, respectively) (Table 3). Washing out the myocardial preparations, the contractility to the pre-drug state was completely retained. This enables us to suppose the effects of our compound as reversible. During the experiment, **4b** did not cause any arrhythmias. Vesnarinone and **4b** increased heart rate by 14 ± 5% and 16 ± 4% at 100 μM, respectively.

Despite the equal inotropic activity of compounds **4b** and vesnarinone, we observed a better selectivity of **4b** toward PDE3A versus PDE3B (0.43 μM vs 1.61 μM) and more inhibitory activity in comparison with vesnarinone by 25 and 8-fold for PDE3A and PDE3B, respectively. Compound **4b** could have an advantage for its clinical application that produces inotropic effect without any obvious change in heart rate. This prevents unnecessary increase in heart oxygen consumption that is an important determinant to exacerbate the heart failure syndrome.

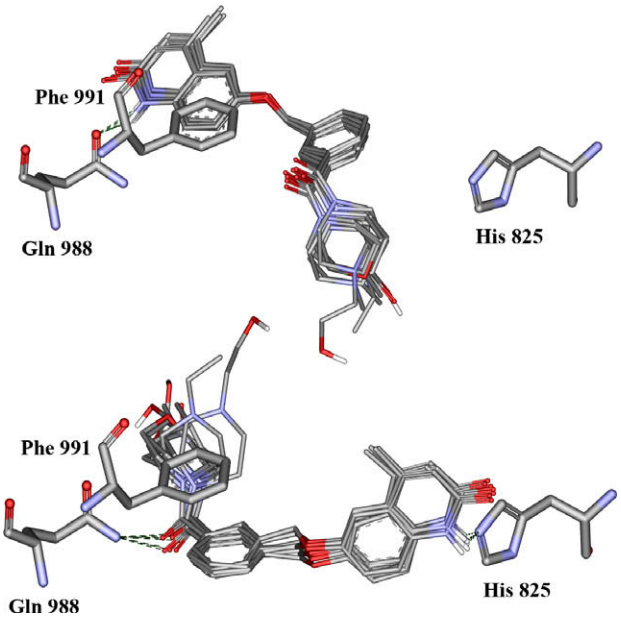


**Figure 4.** Superimposition of the consensus bonding conformations of compounds **4a–j** in the PDE3B active site. The above figure represents the traditional orientation and the below one represents the new proposed orientation.

In summary we have designed and synthesized 3-[(4-methyl-2-oxo-1,2-dihydro-6-quinolinyl)oxy]methylbenzamides **4a–j** as

**Table 2**
Enzyme inhibitory assessment data of compounds **4a–j**, **4a′** and vesnarinone

| Compd | $IC_{50}$ (μM) | |
|---|---|---|
| | PDE3A | PDE3B |
| **4a′** | 2.84 ± 0.05 | 5.67 ± 0.09 |
| **4a** | 1.76 ± 0.03 | 3.51 ± 0.11 |
| **4b** | 1.44 ± 0.04 | 1.93 ± 0.15 |
| **4c** | 1.65 ± 0.02 | 2.80 ± 0.08 |
| **4d** | 1.26 ± 0.06 | 1.14 ± 0.02 |
| **4e** | 0.84 ± 0.06 | 1.28 ± 0.05 |
| **4f** | 1.35 ± 0.05 | 0.91 ± 0.06 |
| **4g** | 0.66 ± 0.03 | 1.73 ± 0.07 |
| **4h** | 0.43 ± 0.04 | 1.61 ± 0.10 |
| **4i** | 1.34 ± 0.03 | 1.54 ± 0.09 |
| **4j** | 0.64 ± 0.05 | 1.20 ± 0.09 |
| Vesnarinone | 10.7 ± 0.09 | 13.2 ± 0.13 |

potent PDE3 inhibitors and inotropic agents. As a conclusion compound **4b** with high inhibitory potency for PDE3A may be a good candidate for treatment of CHF since; in spite of a high efficacy, it may introduce less proarrhythmic side effects.

## 3. Materials and methods

### 3.1. Animals, drugs, chemicals and instruments

Adult male Wistar rats (250–350 g), obtained from animal house of Mashhad medical school, were kept in controlled environmental conditions (temperature: 23 ± 2 °C; light–dark cycle: 7 am to 7 pm). Animals had free access to a standard laboratory diet and water. In order to obtain atrial preparation, depleted in endogenous catecholamine, the animals were treated intraperitoneally with reserpine (5 mg/kg b.wt) 24 h before euthanasia.[28] In each experiment, the animals were anaesthetized with intraperitoneal injection of thiopental 80 mg/kg, and after midline thoracotomy, the heart was rapidly excised and placed in a dissection dish filled with oxygenated Krebs–Henseleit solution. The enzymes were obtained from BPS BioScience Inc. All chemicals purchased from Merck and Fluka Chemical Co.

Melting points were recorded on an Electrothermal type 9100 melting point apparatus. $^1$H NMR (500 MHz) was obtained by using a Bruker Avance DRX-500 Fourier transformer spectrometer. Chemical shifts are reported in ppm ($\delta$) downfield from tetramethylsilane (TMS). Electron impact (EI) mass spectra were recorded on a Varian Match 7A spectrometer. Elemental analysis was obtained on a Thermo Finnigan Flash EA microanalyzer. The developed tension was recorded isometrically by means of a high-sensitivity force transducer (type E. Zimmermann, Eipzig-Berlin) connected to powerlab 8/30 (model 870).

### 3.2. Chemistry

The synthesis of 6-hydroxy-4-methylquinolin-2(1*H*)-one (**1**) and 6-hydroxyquinolin-2(1*H*)-one (**1′**) was reported in last literatures.[29,30] Condensation of **1** and **1′** with methyl-3-(bromomethyl)benzoate in the presence of 1,8-diazabicyclo[5,4,0]undec-7-ene (DBU) afforded the corresponding esters **2** and **2′**.[14] Hydrolysis of **2** and **2′** with HCl 20% gave the corresponding carboxylic acids **3** and **3′**. Various amide derivatives **4a′** and **4a–j** were prepared from various secondary amines and an intermediate acid chloride which was formed from reacting of acids **3** and **3′** with isobutyl chloroformate in the presence of DBU[25] (Scheme 1). Vesnarinone were prepared according to the method reported in previously published work.[31]

### 3.3. Molecular modeling, docking and SAR study

#### 3.3.1. Structure optimization

Structures **4a–j** and vesnarinone were simulated in chem3D professional; Cambridge software; using MM2 method (RMS gradient = 0.05 kcal/mol).[32] Output files were minimized under semi-

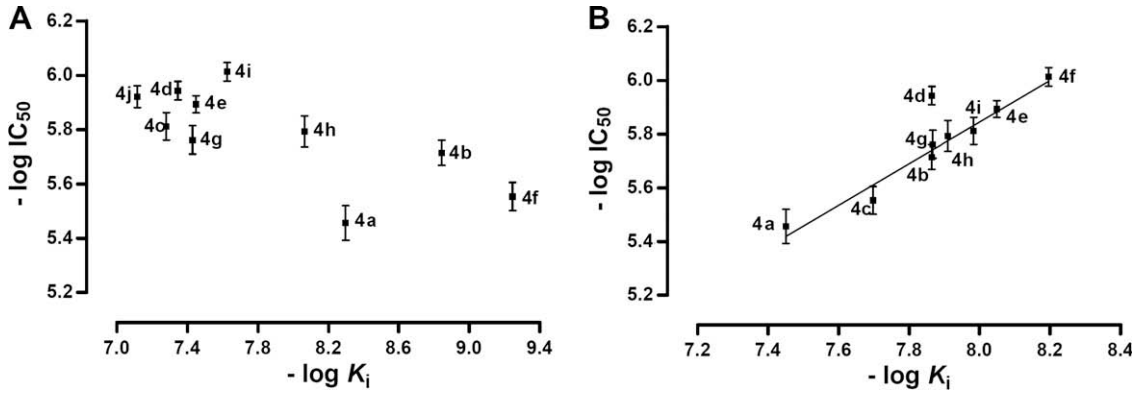


**Figure 5.** Log $IC_{50}$ versus $-\log K_i$ for PDE3B. Diagram A represents the traditional orientation and diagram B represents the new proposed orientation.

**Table 3**
Effects of the compound 4b upon force of contractility and frequency rate of whole atria from reserpine-treated rats in comparison with vesnarinone

| | Compd | Base | $1 \times 10^{-6}$ | $1 \times 10^{-5}$ | $1 \times 10^{-4}$ |
|---|---|---|---|---|---|
| Contractile force | **4b** | 100 ± 3 | 101 ± 2 | 123 ± 2 | 146 ± 3 |
| | Vesnarinone | 100 ± 4 | 102 ± 4 | 121 ± 3 | 141 ± 3 |
| Frequency rate | **4b** | 100 ± 2 | 106 ± 1 | 108 ± 5 | 116 ± 4 |
| | Vesnarinone | 100 ± 3 | 103 ± 7 | 109 ± 6 | 114 ± 5 |

The effect of each concentration (mol $L^{-1}$) of a compound was defined by the difference between the contraction and frequency before and after its addition to the bathing fluid, and was expressed as a percent variation in contraction and frequency in respect to the controls. Results are means ± SEM from six atria.

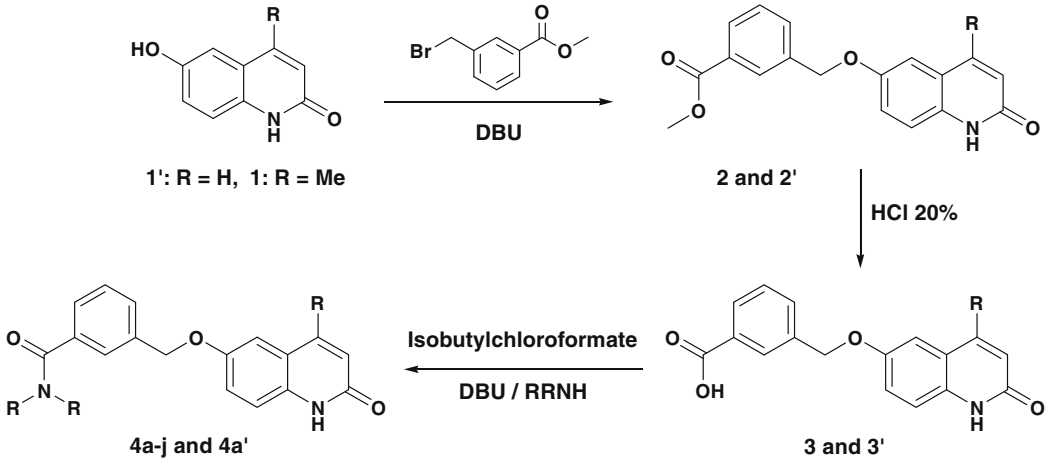


**Scheme 1.** General procedure for the synthesis of compounds **4a–j** and **4a′**.

empirical AM1 method in the second optimization (Convergence limit = 0.01; Iteration limit = 50; RMS gradient = 0.05 kcal/mol; Fletcher–Reeves optimizer algorithm) in HyperChem7.5.[33,34]

Crystal structure of human PDE3B complex with MERCK1 was retrieved from RCSB Protein Data Bank (PDB entry: 1ISO).

### 3.3.2. Molecular docking

Automated docking simulation was implemented to dock **4a–j** into the active site of PDE3B with AutoDockTools 4.0 (ADT4) version 1.5.2[35] using Lamarckian genetic algorithm.[46] This method has been previously shown to produce binding models similar to the experimentally observed models.[16,36,37] The torsion angles of the ligands were identified, hydrogens were added to the macromolecule, bond distances were edited and solvent parameters were added to the enzyme 3D structure. Partial atomic charges were then assigned to the macromolecule as well as ligands (Gasteiger for the ligands and Kollman for the protein).

The regions of interest of the enzyme were defined by considering Cartesian chart 58.4, 2.4 and 10.0 as the central of a grid size of 40, 50 and 40 points in *X*, *Y* and *Z* axises. The docking parameter files were generated using Genetic Algorithm and Local Search Parameters (GALS) while number of generations was set to 100–250. The docked complexes were clustered with a root-mean-square deviation tolerance of 0.2 Å. Autodock generated 100–250 docked conformers of **4a**–**j**-corresponding to the lowest-energy structures. After docking procedure in AD4, docking results were submitted to Accelrys DS Visualizer v2.0.1.7347[38] and Swiss-PdbViewer v3.7b2 (spdbv)[39] for further evaluations. The results of docking processing ($\Delta G_b$: estimated free energy of bonding, $E_d$: final docked energy and $K_i$: estimated inhibition constant) are outlined in Table 1.

### 3.4. Assessment of inotropic and chronotropic activities

The whole atrium was separated from ventricle (for each compounds six atrium was used) and mounted vertically in a 50 ml organ-bath containing Krebs–Henseleit solution constantly gassed by 95% $O_2$ and 5% $CO_2$, 35–37 °C, pH of 7.35–7.45. The bathing solution was made up (in mM): NaCl 118, KCl 4.5, $CaCl_2$ 1.36, $MgSO_4$ 1.21, $NaH_2PO_4$ 1.22, $NaHCO_3$ 25, and glucose 11.[18] Resting tension was adjusted to about 0.5 g in the whole atria[24] and the initial equilibration period was 40–50 min for each preparation. Since the atria were isolated from reserpine-pretreated animals, depletion of catecholamine was verified by lack of any positive inotropic effect induced by tyramine (1.5 μM).[18] Experiments were performed only in preparations that did not response to tyramine. The test compounds were added cumulatively (1–100 μM) and the responses of each concentration were recorded up to the maximum.

### 3.5. Assessment of PDE3A and PDE3B inhibitory activity

Assays were conducted following the instruction from the manufacture of the assay kit. The enzymatic reactions were conducted at room temperature for 60 min in a 50 μl mixture containing IMAP Reaction Buffer, 100 nM FAM-cAMP, 1 ng PDE3A or PDE3B and the test compound.

The binding reactions were performed in the present of Binding Reagent (1:600 dilution in a reagent binding buffer containing 85% Binding Buffer A and 15% Binding Buffer B) at room temperature for 60 min.

Fluorescence intensity was measured at an excitation of 485 nm and an emission of 528 nm using a BioTek Synergy™ 2 microplate reader.

PDE3 activity assays were performed in duplicates at each concentration. Fluorescence intensity is converted to fluorescence polarization using the Gen5 software. The fluorescence polarization data were analyzed using the computer software, Graphpad Prism. The highest value of fluorescence polarization ($FP_t$) in each data set was defined as 100% activity. In the absence of PDE3, the value of fluorescent polarization ($FP_b$) in each data set was defined as 0% activity. The percent activity in the presence of the compound was calculated according to the following equation: %binding = $(FP–FP_b)/(FP_t–FP_b) \times 100$, where FP = the fluorescence polarization in the presence of the compound, $FP_b$ = the fluorescent polarization in the absence of PDE3, and $FP_t$ = the highest fluorescent polarization in each data set.

The $IC_{50}$ values were determined from the % activity of the enzymes at 0.01, 0.1, 1, 10 and 100 μM concentrations of synthetic inhibitors using sigmoidal dose–response curve in Graphpad Prism.

### 3.6. Methyl 3-[(4-methyl-2-oxo-1,2-dihydro-6-quinolinyl)-oxy]methylbenzoate 2

To a solution of 5 g (0.029 mol) of 6-hydroxy-4-methylquinolin-2(1*H*)-one **1** and 6 g of DBU in 80 ml of isopropyl alcohol was added methyl-3-(bromomethyl)benzoate (6.5 g, 0.033 mol) drop-

wise. The mixture was refluxed for 5 h, the solvent was evaporated off, and the residue was extracted with chloroform. After removal of the solvent, the residue was recrystallized from methanol to give **2** as colorless needles (6.8 g, 74%).

White crystal, mp: 190–191 °C; $^1$H NMR ($CDCl_3$): $\delta$ 2.51 (s, 3H, –$CH_3$), 3.98 (s, 3H, $CH_3O$–), 5.20 (s, 2H, –$CH_2O$–), 6.40 (s, 1H, H-3), 7.21 (d, $J$ = 1.8 Hz, 1H, H-5), 7.27 (dd, $J$ = 8.9 Hz, 1.8 Hz, 1H, H-7), 7.43 (d, $J$ = 8.9 Hz, 1H, H-8), 7.52 (t, $J$ = 7.7 Hz, 1H, H-5 (benzoate)), 7.71 (d, $J$ = 7.5, 1H, H-4 (benzoate)), 8.06 (d, $J$ = 7.7, 1H, H-6 (benzoate)), 8.19 (s, 1H, H-2 (benzoate)), 12.33 (s, 1H, NHCO); MS *m/z*: 323 (M+), 321 (100%).

### 3.7. 3-[(4-Methyl-2-oxo-1,2-dihydro-6-quinolinyl)oxy]methylbenzoic acid 3

A suspension of **3** (6 g, 0.019 mol) in 60 ml of 20% HCl was stirred at 85–90 °C for 2 h, and then cooled down to room temperature. The precipitated crystals were collected, and washed with water. The crystals were recrystallized from DMF–water, oven dried gave **3** (5.4 g, 94%).

White crystal, mp: 223–225 °C; $^1$H NMR (DMSO-$d_6$): $\delta$ 2.42 (s, 3H, –$CH_3$), 4.70 (br, COOH & $H_2O$), 5.25 (s, 2H, –$CH_2O$–), 6.46 (s, 1H, H-3), 7.21 (d, $J$ = 1.8 Hz, 1H, H-5), 7.27 (dd, $J$ = 8.9 Hz, 1.8 Hz, 1H, H-7), 7.00–7.29 (m, 3H, H-5, H-7, H-8), 7.45–8.15 (m, 4H, (benzoate)), 11.80 (s, 1H, NHCO); MS *m/z*: 309 (M+), 174 (100%).

### 3.8. General procedure for the synthesis of 4a–j

Isobuthyl chloroformate (1.5 g, 0.011 mol) was added dropwise to a solution of **3** (0.010 mol) and 1.7 g of DBU in 50 ml chloroform while stirring in ice-water. After removing the ice-bath, the reaction mixture was stirred at room temperature for 1 h. the required amine (0.010 mol) was then added dropwise and stirring continued for 3 h. The resulting solution was washed with 0.5 N NaOH (2 × 50 ml), dilute HCl (2 × 50 ml) and water (2 × 50 ml). The organic layer was dried over sodium sulfate. After removing of the solvent under reduced pressure, the residue was recrystallized from acetone to give **4a–j**.

#### 3.8.1. 4-Methyl-6-({3-[(4-methylpiperazino)carbonyl]benzyl}oxy)-1,2-dihydro-2-quinolinone 4a

White crystal, mp: 217–218 °C; $^1$H NMR ($CDCl_3$): $\delta$ 2.35 (m, 5H, $NCH_3$ & –$CH_2NCH_2$– (piperazine)), 2.51 (m, 5H, –$CH_3$ & –$CH_2NCH_2$– (piperazine)), 3.45 (m, 2H, –$CH_2NCOCH_2$– (piperazine)), 3.84 (m, 2H, –$CH_2NCOCH_2$– (piperazine)), 5.18 (s, 2H, –$CH_2O$–), 6.63 (s, 1H, H-3), 7.20 (d, $J$ = 2.6 Hz, 1H, H-5), 7.24 (dd, $J$ = 8.9 Hz, 2.6 Hz, 1H, H-7), 7.40 (d, $J$ = 7.6 Hz, 1H, H-4 (benzoate)), 7.43 (d, $J$ = 8.9 Hz, 1H, H-8), 7.48 (t, $J$ = 7.7 Hz, 1H, H-5 (benzoate)), 7.54–756 (m, 2H, H-2 (benzoate) & H-6 (benzoate)), 12.45 (s, 1H, NHCO); MS *m/z*: 391 (M+), 217 (100%); $C_{23}H_{25}N_3O_3$ requires: C, 70.57; H, 6.44; N, 10.73. Found: C, 70.39; H, 6.41; N, 10.87.

#### 3.8.2. 4-Methyl-6-({3-[(4-ethylpiperazino)carbonyl]benzyl}oxy)-1,2-dihydro-2-quinolinone 4b

White crystal, mp: 193–194 °C; $^1$H NMR ($CDCl_3$): $\delta$ 1.12 (t, $J$ = 7.2 Hz, 3H, $CH_3CH_2N$–), 2.38 (m, 2H, –$CH_2NCH_2$– (piperazine)), 2.47 (q, $J$ = 7.2 Hz, 2H, $CH_3CH_2N$–), 2.51 (m, 3H, –$CH_3$), 2.56 (m, 2H, –$CH_2NCH_2$– (piperazine)), 3.45 (m, 2H, –$CH_2NCOCH_2$– (piperazine)), 3.97 (m, 2H, –$CH_2NCOCH_2$– (piperazine)), 5.19 (s, 2H, –$CH_2O$–), 6.63 (s, 1H, H-3), 7.20 (d, $J$ = 2.6 Hz, 1H, H-5), 7.24 (dd, $J$ = 8.9 Hz, 2.6 Hz, 1H, H-7), 7.39–74.2 (m, 2H, H-8 & H-4 (benzoate)), 7.48 (t, $J$ = 7.7 Hz, 1H, H-5 (benzoate)), 7.54–7.56 (m, 2H, H-2 (benzoate) & H-6 (benzoate)), 12.00 (br, 1H, NHCO); MS *m/z*: 405 (M+), 231 (100%); $C_{24}H_{27}N_3O_3$ requires: C, 71.09; H, 6.71; N, 10.36. Found: C, 71.21; H, 6.81; N, 10.46.

#### 3.8.3. 6-[(3-{[4-(2-Hydroxyethyl)piperazino]carbonyl}-benzyl)oxy]-4-methyl-1,2-dihydro-2-quinolinone 4c

White crystal, mp: 212–213 °C; $^1$H NMR ($CDCl_3$/DMSO-$d_6$): $\delta$ 2.38 (s, 1H, –$CH_3$), 2.52–2.58 (m, 6H, $NCH_2CH_2OH$ & –$CH_2NCH_2$– (piperazine)), 2.98 (s, 1H, –OH), 3.36 (m, 2H, –$CH_2NCOCH_2$– (piperazine)), 3.61 (m, 2H, $NCH_2CH_2OH$), 3.77 (m, 2H, –$CH_2NCOCH_2$– (piperazine)), 5.10 (s, 2H, –$CH_2O$–), 6.46 (s, 1H, H-3), 7.10–7.13 (m, 2H, H-5 & H-7), 7.23 (d, $J$ = 8.7 Hz, 1H, H-8), 7.32 (d, $J$ = 7.6 Hz, 1H, H-4 (benzoate)), 7.41 (t, $J$ = 7.6 Hz, 1H, H-5 (benzoate)), 7.45–7.48 (m, 2H, H-2 (benzoate) & H-6 (benzoate)), 10.91 (s, 1H, NHCO); MS *m/z*: 421 (M+), 247 (100%); $C_{24}H_{27}N_3O_4$ requires: C, 68.39; H, 6.46; N, 9.97. Found: C, 68.49; H, 6.39; N, 9.88.

#### 3.8.4. 4-Methyl-6-(3-[(4-oxopiperidino)carbonyl]benzyloxy)-1,2-dihydro-2-quinolinone 4d

White crystal, mp: 216–217 °C; $^1$H NMR (DMSO-$d_6$): $\delta$ 2.35 (m, 2H, –$CH_2COCH_2$– (piperidone)), 2.41 (s, 3H, –$CH_3$), 2.43 (m, 2H, –$CH_2COCH_2$– (piperidine)), 3.75 (m, 4H, –$CH_2NCOCH_2$– (piperidone)), 5.14 (s, 2H, –$CH_2O$–), 6.37 (s, 1H, H-3), 7.24–7.26 (m, 3H, 1H, H-5 & H-7), 7.33 (d, $J$ = 7.6 Hz, 1H, H-4 (benzoate)), 7.43–7.47 (m, 2H, H-2 & H-5 (benzoate)), 7.56 (m, d, $J$ = 7.6 Hz, 1H, H-6 (benzoate)), 11.59 (s, 1H, NHCO); IR cm$^{-1}$: MS *m/z*: 390 (M+), 216 (100%); $C_{23}H_{22}N_2O_4$ requires: C, 70.75; H, 5.68; N, 7.17. Found: C, 71.00; H, 5.71; N, 7.15.

#### 3.8.5. 1-(3-{[(4-Methyl-2-oxo-1,2-dihydro-6-quinolinyl)oxy]methyl}benzoyl)-4-piperidinecarboxylic acid 4e

White crystal, mp: 236–237 °C; $^1$H NMR (DMSO-$d_6$): $\delta$ 1.50 (m, 2H, –$CH_2CHCH_2$– (piperidine)), 1.70–2.00 (m, 2H, –$CH_2CHCH_2$– (piperidine)), 2.39 (s, 3H, –$CH_3$), 2.54 (m, 1H, –CH– (piperidine)), 2.90–3.20 (m, 2H, –$CH_2NCOCH_2$– (piperidine)), 3.51 (m, 1H, –$CH_2NCOCH_2$– (piperidine)), 4.35 (m, 1H, –$CH_2NCOCH_2$– (piperidine)), 5.22 (s, 2H, –$CH_2O$–), 6.39 (s, 1H, H-3), 7.25–7.27 (m, 3H, 1H, H-5 & H-7), 7.33 (d, $J$ = 7.6 Hz, 1H, H-4 (benzoate)), 7.46–7.49 (m, 2H, H-2 & H-5 (benzoate)), 7.55 (m, d, $J$ = 7.6 Hz, 1H, H-6 (benzoate)), 11.48 (s, 1H, NHCO), 12.35 (s, 1H, -COOH); IR cm$^{-1}$: MS *m/z*: 420 (M+), 246 (100%); $C_{24}H_{24}N_2O_5$ requires: C, 68.56; H, 5.75; N, 6.66. Found: C, 68.37; H, 5.71; N, 6.72.

#### 3.8.6. 6-({3-[(4-Hydroxypiperidino)carbonyl]benzyl}oxy)-4-methyl-1,2-dihydro-2-quinolinone 4f

White crystal, mp: 251–252 °C; $^1$H NMR (DMSO-$d_6$): $\delta$ 1.20–1.50 (m, 2H, –$CH_2CHCH_2$– (piperidine)), 1.60–1.90 (m, 2H, –$CH_2CHCH_2$– (piperidine)), 2.39 (s, 3H, –$CH_3$), 3.00–3.30 (m, 2H, -$CH_2NCOCH_2$- (piperidine)), 3.44 (m, 1H, –$CH_2NCOCH_2$– (piperidine)), 3.73 (m, 1H, –CH– (piperidine)), 4.01 (m, 1H, –$CH_2NCOCH_2$– (piperidine)), 4.78 (d, $J$ = 4.0 Hz, 1H, –OH (piperidine)), 5.22 (s, 2H, –$CH_2O$–), 6.39 (s, 1H, H-3), 7.25–7.27 (m, 3H, 1H, H-5 & H-7), 7.33 (d, $J$ = 7.6 Hz, 1H, H-4 (benzoate)), 7.45–7.48 (m, 2H, H-2 & H-5 (benzoate)), 7.55 (m, d, $J$ = 7.6 Hz, 1H, H-6 (benzoate)), 11.49 (s, 1H, NHCO); MS *m/z*: 392 (M+), 218 (100%); $C_{23}H_{24}N_2O_4$ requires: C, 70.39; H, 6.16; N, 7.14. Found: C, 70.29; H, 6.11; N, 7.18.

#### 3.8.7. 4-Methyl-6-{[3-(piperidinocarbonyl)benzyl]oxy}-1,2-dihydro-2-quinolinone 4g

White crystal, mp: 200–201 °C; $^1$H NMR ($CDCl_3$/DMSO-$d_6$): $\delta$ 1.63 (m, 1H, –$CH_2CH_2CH_2$– (piperidine)), 1.71 (m, 4H, –$CH_2CH_2CH_2$– (piperidine)), 1.88 (m, 1H, –$CH_2CH_2CH_2$– (piperidine)), 2.50 (s, 3H, –$CH_3$), 3.28 (t, $J$ = 5.1 Hz, 2H, –$CH_2NCOCH_2$– (piperidine)), 3.36 ((t, $J$ = 5.1 Hz, 2H, –$CH_2NCOCH_2$– (piperidine)), 5.18 (s, 2H, –$CH_2O$–), 6.62 (s, 1H, H-3), 7.19 (d, $J$ = 2.5 Hz, 1H, H-5), 7.24 (dd, $J$ = 8.7 Hz, 2.5 Hz, 1H, H-7), 7.37–741 (m, 2H, H-8 & H-4 (benzoate)), 7.46 (t, $J$ = 7.5 Hz, 1H, H-5 (benzoate)), 7.52–7.54 (m, 2H, H-2 (benzoate) & H-6 (benzoate)), 11.33 (s, 1H, NHCO); MS *m/z*: 376 (M+), 202 (100%); $C_{23}H_{24}N_2O_3$ requires: C, 73.38; H, 6.43; N, 7.44. Found: C, 72.89; H, 6.41; N, 7.51.

### 3.8.8. 4-Methyl-6-({3-[(4-methylpiperidino)carbonyl]-benzyl}oxy)-1,2-dihydro-2-quinolinone 4h

White crystal, mp: 230–231 °C; $^1$H NMR ($CDCl_3$): $\delta$ 0.84 (d, $J$ = 6.4, 3H, –$CH_3$ (piperidine)), 0.91 (m, 1H, –$CH_2$CH$CH_2$– (piperidine)), 1.11 (m, 1H, –$CH_2$CH$CH_2$– (piperidine)), 1.44 (m, 1H, –$CH_2$CH$CH_2$– (piperidine)), 1.55 (m, 1H, –$CH_2CH$CH$_2$– (piperidine)), 1.67 (m, 1H, –$CH_2$CH$CH_2$– (piperidine)), 2.34 (s, 3H, –$CH_3$), 2.67 (m, 1H, –$CH_2$NCOCH$_2$– (piperidine)), 2.87 (m, 1H, –$CH_2$NCOCH$_2$– (piperidine)), 3.56 (m, 1H, –$CH_2$NCOCH$_2$– (piperidine)), 4.52 ((m, 1H, –$CH_2$NCOCH$_2$– (piperidine)), 5.05 (s, 2H, –$CH_2$O–), 6.41 (s, 1H, H-3), 7.05 (d, $J$ = 2.5 Hz, 1H, H-5), 7.07 (dd, $J$ = 8.7 Hz, 2.5 Hz, 1H, H-7), 7.19–7.25 (m, 2H, H-8 & H-4 (benzoate)), 7.31 (t, $J$ = 7.6 Hz, 1H, H-5 (benzoate)), 7.37–741 (m, 2H, H-2 (benzoate) & H-6 (benzoate)), 11.52 (s, 1H, NHCO); MS *m/z*: 390 (M+), 216 (100%); $C_{24}H_{26}N_2O_3$ requires: C, 73.82; H, 6.71; N, 7.17. Found: C, 73.57; H, 6.64; N, 7.09.

### 3.8.9. 4-Methyl-6-{[3-(morpholinocarbonyl)benzyl]oxy}-1,2-dihydro-2-quinolinone 4i

White crystal, mp: 211–212 °C; $^1$H NMR ($CDCl_3$): $\delta$ 2.51 (s, 3H, –$CH_3$), 3.48–3.81 (m, 8H, (morpholin)), 5.18 (s, 2H, –$CH_2$O–), 6.41 (s, 1H, H-3), 7.21 (d, $J$ = 2.6 Hz, 1H, H-5), 7.25 (dd, $J$ = 8.7 Hz, 2.6 Hz, 1H, H-7), 7.40–7.43 (m, 2H, H-8 & H-4 (benzoate)), 7.31 (t, $J$ = 7.7 Hz, 1H, H-5 (benzoate)), 7.56–758 (m, 2H, H-2 (benzoate) & H-6 (benzoate)), 12.32 (s, 1H, NHCO); MS *m/z*: 378 (M+), 204 (100%); $C_{22}H_{22}N_2O_4$ requires: C, 69.83; H, 5.86; N, 7.40. Found: C, 69.77; H, 5.84; N, 7.51.

### 3.8.10. 4-Methyl-6-{[3-(tetrahydro-1*H*-1-pyrrolylcarbonyl)-benzyl]oxy}-1,2-dihydro-2-quinolinone 4j

White crystal, mp: 193–194 °C; $^1$H NMR ($CDCl_3$): $\delta$ 1.90 (m, 2H, –$CH_2CH_2$– (pyrrolydine)), 2.00 (m, 2H, –$CH_2CH_2$– (pyrrolydine)), 2.51 (s, 3H, $CH_3$–), 3.43 (t, $J$ = 6.6 Hz, 2H, –$CH_2$NCOCH$_2$– (pyrrolydine)), 3.69 t, $J$ = 6.6 Hz, 2H, –$CH_2$NCOCH$_2$– (pyrrolydine)), 5.18 (s, 2H, –$CH_2$O–), 6.63 (s, 1H, H-3), 7.20 (d, $J$ = 2.6 Hz, 1H, H-5), 7.25 (dd, $J$ = 8.9 Hz, 2.6 Hz, 1H, H-7), 7.41 (d, $J$ = 8.9 Hz, 1H, H-8), 7.48 (d, $J$ = 7.5 Hz, 1H, H-4 (benzoate)), 7.52–7.55 m, 2H, H-5 (benzoate) & H-6 (benzoate)), 767 (s, 1H, H-2 (benzoate)), 12.19 (s, 1H, NHCO); MS *m/z*: 362 (M+), 188 (100%); $C_{22}H_{22}N_2O_3$ requires: C, 72.91; H, 6.12; N, 7.73. Found: C, 72.77; H, 6.10; N, 7.81.

### 3.9. General procedure for the synthesis of 4a′

The synthetic pathway for the total synthesis of **4a′**, by starting from **1′**, is same as which was reported for **4a–j**.

### 3.9.1. 4-Methyl-6-({3-[(4-methylpiperazino)carbonyl]-benzyl}oxy)-1,2-dihydro-2-quinolinone 4a′

White crystal, mp: 227–228 °C; $^1$H NMR ($CDCl_3$): $\delta$ 2.38 (m, 5H, $NCH_3$ & –$CH_2NCH_2$– (piperazine)), 2.55 (m, 2H, –$CH_2NCH_2$– (piperazine)), 3.49 (m, 2H, –$CH_2$NCOCH$_2$– (piperazine)), 3.87 (m, 2H, –$CH_2$NCOCH$_2$– (piperazine)), 5.15 (s, 2H, –$CH_2$O–), 6.62 (d, $J$ = 8.8, 1H, H-3), 7.20 (d, $J$ = 2.6 Hz, 1H, H-5), 7.24 (dd, $J$ = 8.9 Hz, 2.6 Hz, 1H, H-7), 7.41 (d, $J$ = 7.7 Hz, 1H, H-4 (benzoate)), 7.41 (d, $J$ = 8.8 Hz, 1H, H-8), 7.44 (t, $J$ = 7.6 Hz, 1H, H-5 (benzoate)), 7.48–754 (m, 2H, H-2 (benzoate) & H-6 (benzoate)), 7.66 (d, $J$ = 8.8 Hz, 1H, H-4), 12.45 (s, 1H, NHCO); MS *m/z*: 377 (M+), 217 (100%); $C_{23}H_{25}N_3O_3$ requires: C, 70.01; H, 6.14; N, 11.13. Found: C, 70.22; H, 6.21; N, 10.99.

## Acknowledgments

We express our sincere gratitude to Dr. Hossein Orafaie and Mohammad Naser Shafiee for reviewing the manuscript. We are also grateful to BPS Bioscience Inc. for enzyme assays.

## References and notes

1. Beavo, J. A. *Physiol. Rev.* **1995**, *75*, 725.
2. Nicholson, C. D.; Challiss, R. A. J.; Shahid, M. *Trends Pharmacol. Sci.* **1991**, *12*, 19.
3. Polson, J. B.; Strada, S. J. *Annu. Rev. Pharmacol. Toxicol.* **1996**, *36*, 403.
4. Rose, R. J.; Liu, H.; Palmer, D.; Maurice, D. H. *Br. J. Pharmacol.* **1997**, *122*, 233.
5. Reeves, M. L.; Leigh, B. K.; England, P. J. *Biochem. J.* **1987**, *241*, 535.
6. Hidaka, H.; Asano, T. *Biochim. Biophys. Acta.* **1976**, *429*, 485.
7. Hidaka, H.; Hayashi, H.; Kohri, H.; Kimur, H.; Hosokawa, T.; Igawa, T. *J. Pharmacol. Exp. Ther.* **1979**, *211*, 26.
8. Souness, J. E.; Hassall, G. A.; Parrott, D. P. *Biochem. Pharmacol.* **1992**, *44*, 857.
9. Reinhardt, R. R.; Chin, E.; Zhou, J.; Taira, M.; Murata, T.; Manganiello, V. C.; Bondy, C. A. *J. Clin. Invest.* **1995**, *95*, 1528.
10. Palmer, D.; Maurice, D. H. *Mol. Pharmacol.* **2000**, *58*, 247.
11. Tominaga, M.; Yo, E.; Ogava, H.; Yamashita, S.; Yabuuchi, Y.; Nakagava, K. *Chem. Pharm. Bull.* **1984**, *32*, 2100.
12. Yamashita, S.; Hosokawa, T.; Kojima, M.; Mori, T.; Yabuuchi, Y. *Arzneimittelforschung* **1984**, *34*, 342.
13. Feldman, A. M. *Cardiovasc. Drug Rev.* **1993**, *11*, 1.
14. Kavamata, H.; Nakashiro, K.; Uchida, D. *Br. J. Cancer* **1998**, *77*, 71.
15. Kondo, T.; Suzuki, Y.; Kitano, T.; Iwai, K.; Watanabe, M.; Umehara, H.; Daido, N.; Domae, N.; Tashima, M.; Uchiyama, T.; Okazaki, T. *Mol. Pharmacol.* **2002**, *61*, 620.
16. Dym, O.; Xenarios, I.; Ke, H.; Colicelli, J. *Mol. Pharmacol.* **2002**, *61*, 20.
17. Zhang, W.; Ke, H.; Colman, R. W. *Mol. Pharmacol.* **2002**, *62*, 514.
18. Fossa, P.; Menozzi, G.; Dorigo, P.; Floreani, M.; Mosti, L. *Bioorg. Med. Chem.* **2003**, *11*, 4749.
19. Scapin, G.; Patel, S. B.; Chung, C.; Varnerin, J. P.; Edmondson, S. D.; Mastracchio, A.; Parmee, E. R.; Singh, S. B.; Becker, J. W.; Van der Ploeg, L.; Tota, M. R. *Biochemistry* **2004**, *43*, 6091.
20. Cheung, P. P.; Yu, L.; Zhang, H.; Colman, R. W. *Arch. Biochem. Biophys.* **1998**, *360*, 99.
21. Zhang, W.; Colman, R. W. *Blood* **2000**, *95*, 3380.
22. Zhang, W.; Ke, H.; Tretiakova, A. P.; Jameson, B.; Colman, R. W. *Protein Sci.* **2001**, *10*, 1481.
23. Chung, C.; Varnerin, J.; Morin, N. R.; MacNeil, D. J.; Singh, S. B.; Patel, S.; Scapin, G.; Van der Ploeg, L.; Tota, M. R. *Biochem. Biophys. Res. Commun.* **2003**, *307*, 1045.
24. http://www.ncbi.nlm.nih.gov/BLAST/Blast.cgi.
25. Altschul, S. F.; Madden, T. L.; Schäffer, A. A.; Zhang, J.; Zhang, Z.; Miller, W.; Lipman, D. J. *Nucleic Acids Res.* **1997**, *25*, 3389.
26. Schäffer, A. A.; Aravind, L.; Madden, T. L.; Shavirin, S.; Spouge, J. L.; Wolf, Y. I.; Koonin, E. V.; Altschul, S. F. *Nucleic Acids Res.* **2001**, *29*, 2994.
27. Sadeghian, H.; Seyedi, S. M.; Saberi, M. R.; Shafiee Nick, R.; Hosseini, A.; Bakavoli, M.; Mansouri, S. M. T.; Parsaee, H. J. *Enzyme Inhib. Med. Chem.* **2009**, *24*, 918.
28. Martinez, E.; Penaafiel, R.; Collado, M. C.; Hernaandez, J. *Eur. J. Pharmacol.* **1995**, *282*, 169.
29. Campbell, K. N.; Tipson, R. S.; Elderfield, R. C.; Campbell, B. K.; Clapp, M. A.; Gensler, Y. J.; Morrison, D.; Moran, W. J. *J. Org. Chem.* **1946**, *11*, 803.
30. Holmes, R. R.; Conrady, J.; Guthrie, J.; Mckay, R. *J. Am. Chem. Soc.* **1954**, *76*, 2400.
31. Tominaga, M.; Yo, E.; Ogawa, H.; Yamashita, S.; Yabuuchi, Y.; Nakagawa, K. *Chem. Pharm. Bull.* **1984**, *32*, 2100.
32. ChemDraw® Ultra, *Chemical Structure Drawing Standard*, CambridgeSoft Corporation, 100 Cambridge Park Drive, Cambridge, MA 02140, USA, http://www.cambrigesoft.com.
33. HyperChem® Release 7, Hypercube Inc., http://www.hyper.com/.
34. Sadeghian, H.; Seyedi, S. M.; Saberi, M. R.; Arghiani, Z.; Riazi, M. *Bioorg. Med. Chem.* **2008**, *16*, 890.
35. Auto Dock Tools (ADT), The Scripps Research Institute, 10550 North Torrey Pines Road, La Jolla, CA 92037-1000, USA; Python, M. F. S. A programming language for software integration and development. *J. Mol. Graphics Mod.* **1999**, *17*, 57–61.
36. Sadeghian, H.; Attaran, N.; Jafari, Z.; Saberi, M. R.; Pordel, M.; Riazi, M. M. *Bioorg. Med. Chem.* **2009**, *17*, 2327.
37. Sippl, W. *J. Comput. Aided Mol. Des.* **2000**, *14*, 559.
38. http://accelrys.com/products/discovery-studio.
39. Swiss-pdbViewer 3.6, Glaxo Wellcome Experimental Research, http://www.expasy.org/spdbv.